

Structure and Bonding in a Series of Neutral and Cationic Transition Metal–Benzene η^6 Complexes $[M(\eta^6\text{-C}_6\text{H}_6)]^{n+}$ (M = Ti, V, Cr, Fe, Co, Ni, and Cu). Correlation of Charge Transfer with the Bathochromic Shift of the E_1 Ring Vibration

Patrick Chaquin,^{*,†} Dominique Costa,[‡] Christine Lepetit,[§] and Michel Che^{‡,||}

Laboratoire de Chime Théorique, UMR 7616 Université Pierre et Marie Curie-CNRS, Box 137, 4, Place Jussieu, 75252 Paris Cedex 05, France, Laboratoire de Réactivité de Surface, UMR 7609, Université Pierre et Marie Curie-CNRS, Box 176, 4, Place Jussieu, 75252 Paris Cedex 05, France, Laboratoire de Chimie de Coordination, UPR 8241 CNRS, 205, route de Narbonne, 31077 Toulouse, France, and Institut Universitaire de France

Received: November 22, 2000; In Final Form: February 23, 2001

Geometries and bonding energies have been calculated at the B3LYP/3-21G** and B3LYP/DZVP2 levels in a series of $[M(\eta^6\text{-C}_6\text{H}_6)]^{n+}$ complexes where M = Ti, Cr, Co ($n = 0$), V ($n = 3$), Fe ($n = 0, 2$), Ni ($n = 0, 2, 4$), and Cu ($n = 1$) with C_{6v} or near C_{6v} symmetry. Metal–benzene bonding is discussed on the basis of MO perturbation schemes. A correlation between the total benzene charge and the frequency shift of the E_1 ring vibration (experimentally at 1483 cm^{-1} for isolated benzene) is evidenced, allowing interpretation of experimental data.

Introduction

Oxide-supported transition metal complexes constitute a broad class of heterogeneous catalysts. Among them, benzene complexes are of a double interest; they are potential intermediates in catalytic processes (such as partial or total hydrogenation of benzene¹), and from this point of view it is important to know the nature of the metal–benzene interaction and the structure, especially the hapticity, of the benzene. From another point of view, the benzene ligand constitutes a probe molecule which allows us to obtain information on the nature of the catalytic site. As a matter of fact, its IR spectrum exhibits an intense ring E_1 ν_{CC} absorption band in the 1450 cm^{-1} region, which is sensitive to the strength and hapticity of the benzene–metal interaction.^{2–4}

After a previous study of systems including a model of a silica support with a nickel atom in various oxidation states and benzene,³ it was interesting to obtain a deeper insight into the nature of benzene–metal interaction as a function of the nature of the metal and of its oxidation state. Such a study is of interest in other areas of chemistry; uncharged metal–benzene aggregates can be prepared in inert matrixes,⁴ whereas monocation and, more recently, doubly charged compounds can be formed and studied in MS-MS experiments.⁵ Some complexes with a single or several positive charges can exist in interstellar space and are involved in metal depletion.⁶

Some recent experimental and theoretical studies on $M(\text{C}_6\text{H}_6)$ complexes are available in the literature. Alkaline,⁷ alkaline earth⁸ and aluminum⁹ metal–benzene systems have been investigated. In the transition metal area, Bauschlicher et al.¹⁰

presented results of MCPFDZP calculations on the first series monocation complexes, restricted to C_{6v} symmetry; recently the same series was studied by Yang and Klippenstein¹¹ by various methods including the B3LYP DFT. The comparison of the binding energies calculated by both methods evidenced the accuracy of the B3LYP functional for this kind of system. Binding energies, geometry optimization, and in some cases vibration frequencies have also been reported for Cr and Cr^+ ,¹² V and V^+ ,¹³ Fe⁺, and Co^+ .¹⁴ In the present work, we have investigated $M(\eta^6\text{-C}_6\text{H}_6)^{n+}$ compounds involving the first transition metal period. (Let us recall that, according to the hapticity nomenclature, η^6 means that the metal is linked to all six atoms of benzene ligand). The metals have been chosen to provide a wide sampling of situations. For example, the sequence Ti^0 , Cr^0 , Fe^0 , Co^0 , Ni^0 , and Cu^0 allows us to study the influence of the nature of the metal along the period, with variation of the electronegativity together with the number of d electrons, whereas in the isoelectronic series Cr^0 , Fe^{2+} , and Ni^{4+} , the main parameter of concern is the energy level of d atomic orbitals (AOs).

To compare different systems, we have avoided those which exhibit strong Jahn–Teller distortions resulting in the loss of degeneracy of the E_1 vibration mode of interest.¹⁵ For each system, we only have considered the lowest state of each spin multiplicity, whenever it has been possible to optimize a η^6 structure. Nevertheless, a low-lying singlet excited state of $\text{Ti}(\text{C}_6\text{H}_6)^0$ has been described. The rather unrealistic Ni^{4+} and V^{3+} complexes have been included in our study as examples of strong benzene-to-metal electron transfers.

We will present an overview of the benzene–metal interactions, and a qualitative discussion of the main trends on the basis of DFT calculations. In particular, we will study the consequences of these interactions on the E_1 ring vibration frequency, experimentally observed at 1483 cm^{-1} for isolated benzene.¹⁶

* Author to whom correspondence should be addressed.

[†] Laboratoire de Chime Théorique, UMR 7616 Université Pierre et Marie Curie-CNRS.

[‡] Laboratoire de Réactivité de Surface, UMR 7609 Université Pierre et Marie Curie-CNRS.

[§] Laboratoire de Chimie de Coordination, UPR 8241 CNRS.

^{||} Institut Universitaire de France.

TABLE 1: Energy, Main Geometrical Parameters, and Bonding Energy of Metal–Benzene Complexes (a) Bonding Energies E_b are Calculated at the DZVP2 Level with Respect to the Sum of the Energies of Isolated Neutral Benzene and Metal Atom or Ion with the Same Charge and Multiplicity as the Whole Complex

metal	energy (Hartrees)		C–C (Å)		M–C (Å)		E_b^a (kcal mol ⁻¹)
	3-21 G*	DZVP2	3-21 G*	DZVP2	3-21G*	DZVP2	
⁵ Ti ⁰	-1076.264163	-1081.571739	1.424	1.420	2.345	2.401	27.7
¹ Ti ⁰	-1076.218281	-1081.547856	1.459	1.447	2.106	2.148	46.2
¹ Cr ⁰	-1270.310646	-1276.525047	1.443	1.437	2.030	2.071	71.2
³ Fe ⁰	-1488.605682	-1495.772433	1.444	1.434	2.012	2.081	71.2
¹ Fe ²⁺	-1487.842891	-1495.040174	1.415–1.434	1.423–1.424	2.102–2.123	2.115–2.116	29.9
² Co ⁰	-1667.054050	-1614.800339	1.440–1.441	1.430–1.433	1.984–1.986	2.065–2.072	208.2
¹ Ni ⁰	-1732.004143	-1740.333059	1.438	1.430	1.963	2.061	12.7
³ Ni ²⁺	-1731.313847	-1739.630750	1.425	1.425	2.168	2.239	45.8
¹ Ni ⁴⁺	-1729.568280	-1737.889533	1.471	1.469	2.391–2.026	2.430–2.190	193.4
¹ Cu ⁺	-1863.323209	-1872.274805	1.427	1.418	2.042	2.270	2032.0 58.4

Calculation Methods

The GAUSSIAN 94 series of programs¹⁷ has been used throughout this work. Full geometry optimizations and frequency calculations were performed at the DFT level using Becke's three parameters functional¹⁸ with correlation functional of Lee, Yang, and Parr¹⁹ (B3LYP). The results are reported on with two basis sets: the standard 3-21G* and a double- ζ plus polarization (DZVP2) designed for DFT calculations.²⁰ For open shell species, the spin-unrestricted determinant has been used, except for Co⁰ for which the results are given with a spin-restricted determinant (see discussion below).

We present the results relative to Ni⁴⁺ and V³⁺ with a word of caution. First, the standard basis sets used here are optimized for neutral metals and thus could be inadequate; and secondly, Davidson pointed out the failures of correlation functionals in highly charged species.²¹

Results and Discussion

Table 1 reports on the main geometrical parameters of the various complexes, absolute energies, and bonding energies with respect to their asymptotic value of the state energy, i.e., benzene plus metal or ion of the same charge and multiplicity as the complex. These values are reported, rather than the classical bonding energy (with respect to the metal ground state), as straightforward indices of the metal–benzene interaction, independent from the energy separation of the various electronic states of metal atoms or ions.

In all cases we observe a stretching of the C–C bonds with respect to isolated benzene, the bond lengths of which are 1.397 and 1.402 Å at the 3-21G* and DZVP2 levels, respectively. The C–C bonds are generally longer and thus weaker in uncharged complexes, with a maximum for ¹Ti⁰ (1.459 and 1.447 Å depending on the basis set). These bonds are on the contrary shorter in the charged complexes of late transition metals such as ¹Fe²⁺, ³Ni²⁺, and ¹Cu⁺.

The general qualitative MO perturbation scheme is displayed in Figure 1. When interacting with benzene orbitals, the d set of metal atomic orbitals (AOs) is split into three levels of e₂, a₁, and e₁ symmetry, respectively.

The e₁ (*xz* and *yz*) degenerate couple is destabilized by antibonding mixing with the π_2 and π_3 HOMOs of benzene which are on the contrary stabilized by the corresponding bonding mixing. This interaction corresponds to a strong overlap and thus is likely to contribute to a covalent bonding if the antibonding *xz* and *yz* levels are empty. This bonding decreases as the number of electrons in these levels increases. If this MO set is not filled, the interaction results in a benzene-to-metal electron transfer. An additional stabilizing interaction with 4p_x

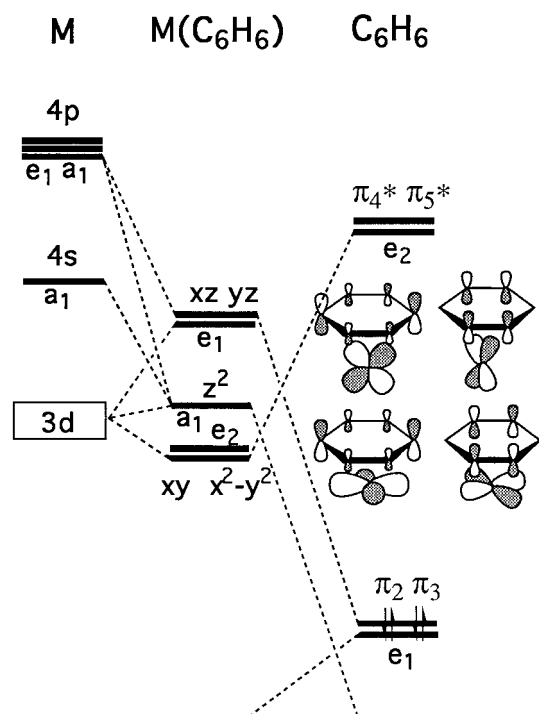


Figure 1. Benzene–metal MO perturbation scheme.

and 4p_y occurs, which increases as the level of these metal AOs decreases and becomes closer to π_2 , π_3 .

The a₁ (*z*²) AO is weakly destabilized by low-lying π and σ MOs of benzene and undergoes a stabilizing interaction by hybridization with 4s and 4p_z of the same symmetry.

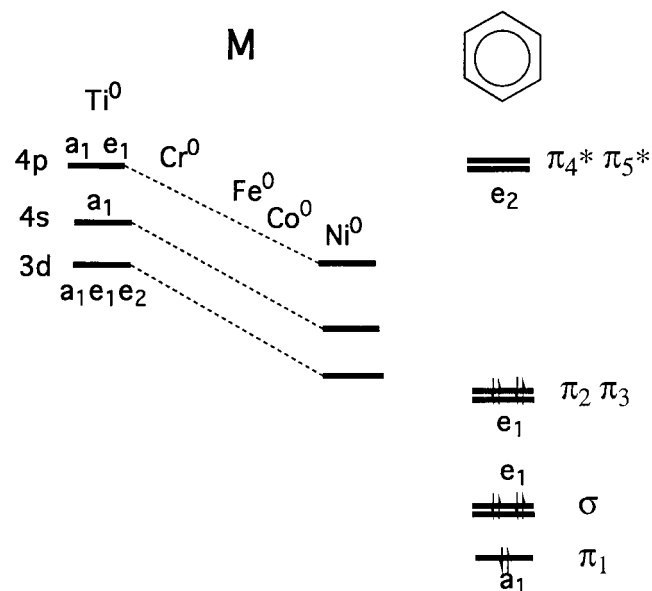
The e₂ set (*x*²–*y*² and *xy*) poorly overlaps with antibonding π_4^* and π_5^* MOs of benzene. This interaction cannot contribute efficiently to covalent bonding but may result in a metal-to-benzene charge transfer if electrons are present in the metal AOs of concern. In fact, a₁ and e₂ levels are close one to another and, according to their occupancy and to the nature of the metal, may be inverted.

The relative importance of the various interactions described in the previous section depends on the energy differences of the interacting levels. Two cases can be considered: neutral metals, having a valence shell lying roughly between the HOMOs and the LUMOs of benzene, and cations having a valence shell nearby or below the benzene HOMOs, with more contracted orbitals as those of neutral metal atoms.

Metal–Benzene Bonding in Neutral Complexes. The relative changes in the metal and benzene levels along the series Ti⁰–Ni⁰ is shown in Figure 2. Indeed, with ¹Ti and ¹Cr complexes of respective configuration e₂⁴ and e₂⁴a₁², the e₁ *xz*

TABLE 2: Total Benzene Mulliken Charge (q , atomic units) and Bathochromic Shift ($\Delta\nu$, cm^{-1}) in the E_1 Vibration Frequency of Benzene in $M(\text{C}_6\text{H}_6)$ Complexes at the B3LYP/3-21G* Level

M	${}^5\text{Ti}^0$	${}^1\text{Ti}^0$	${}^1\text{Cr}^0$	${}^3\text{Fe}^0$	${}^2\text{Co}^0$	${}^1\text{Ni}^0$	${}^1\text{Cu}^+$	${}^1\text{Fe}^{2+}$	${}^3\text{Ni}^{2+}$	${}^1\text{Ni}^{4+}$	${}^1\text{V}^{3+}$
q	-0.53	-1.37	-1.25	-1.01	-0.86	-0.74	0.04	0.47	0.66	2.20	1.14
$\Delta\nu$	44.5	127	93	92	74	60	32	38	33	186	55–75

**Figure 2.** Qualitative variation of the relative orbital energies of benzene and metal along the series Ti^0 – Ni^0 .

and yz level are empty and the π^2, π^3 – xz, yz interaction leads to a maximum stabilization, with four bonding electrons. Moreover, this interaction is greater with Cr which has lower d AOs, accounting for the relative bonding energies for $[\text{Ti}(\text{C}_6\text{H}_6)]^0$ (46.2 kcal mol $^{-1}$) and $[\text{Cr}(\text{C}_6\text{H}_6)]^0$ (71.2 kcal mol $^{-1}$). Quintet ${}^5\text{Ti}^0$ complex has a configuration $a_1^1 e_2^2 a_1^1$ different from that expected from Figure 1. The lowest a_1 MO is mainly z^2 , stabilized by mixing of 4s and $4p_z$, and the highest a_1 level has a dominant $4s + 4p_z$ character. As a result, the e_1 levels remain empty and the bonding is essentially the same as in the singlet ${}^1\text{Ti}^0$ complex. The $[\text{Ti}(\text{C}_6\text{H}_6)]^0$ complex is more stable than $[\text{Ti}(\text{C}_6\text{H}_6)]^0$ by 14.9 kcal mol $^{-1}$ essentially due to high spin stabilization. Its bonding energy, with respect to the ${}^5\text{Ti}^0$ atom plus benzene is only 27.7 kcal mol $^{-1}$ since MOs of higher energy must be occupied to reach the quintet multiplicity.

In the $[\text{Fe}(\text{C}_6\text{H}_6)]^0$ complex, two electrons are present in the antibonding e_1 level yielding a bonding energy drop of 29.9 kcal mol $^{-1}$.

The $[\text{Co}(\text{C}_6\text{H}_6)]^0$ complex exhibits, at the B3LYP/3-21G* and B3LYP/DZVP2 levels using a spin-unrestricted determinant, a $e_2^4 a_1^2 e_1^3$ configuration and a C_{2v} symmetry due to a Jahn–Teller distortion, with M–C distances in the range 1.984–1.987 Å. Nevertheless, at the B3LYP/3-21G* level using a spin-restricted determinant, the configuration is $e_2^2 e_1^4 a_1^1$ and the complex becomes C_{6v} . In all cases, the energy difference between these C_{2v} and C_{6v} geometries is small, ca. 4 kcal mol $^{-1}$. Depending on the case, 3 or 4 electrons are present in the antibonding e_1 levels and the bonding energy is low, 12.7 kcal mol $^{-1}$ at the RB3LYP/DZVP2 level.

The $[\text{Ni}(\text{C}_6\text{H}_6)]^0$ complex, with a $e_2^4 a_1^2 e_1^4$ configuration has an unexpectedly high bonding energy of 45.8 kcal mol $^{-1}$ with respect to benzene plus ${}^1\text{Ni}^0$. A larger participation of 4s and 4p AOs (closer in energy to benzene MOs than for the preceding metals) could explain this value. Let us nevertheless

remember that the ground state of Ni is not singlet, but triplet: the bonding energy is only 13.7 kcal mol $^{-1}$ with respect to ${}^3\text{Ni}^0$ atom.

Beside the e_1 interactions which are the main contribution to covalent bonding between metal and benzene, the weak overlap between xy , x^2-y^2 , and π_4^* , π_5^* (e_2 symmetry) takes place, resulting in a metal-to-benzene electron transfer and to an essentially ionic contribution to the bonding. This interaction is maximum with ${}^1\text{Ti}^0$ yielding a fully occupied e_2 set and the energy gap between these orbitals is weak. It decreases along the series as the 3d– π^* gap increases. An intermediate situation is encountered in the ${}^5\text{Ti}^0$ –benzene interaction with a small energy gap, but only a half-filled e_2 set. The overall electron transfer will be discussed later on.

Metal–Benzene Bonding in Cationic Complexes. In the ${}^1\text{Cu}^+$ complex, isoelectronic to the Ni^0 one, the calculated C–C and M–C bond lengths of 1.414 and 2.270 Å (DZVP2), respectively, are in good agreement with Yang and Klippenstein’s values (1.418 and 2.326).¹¹ The xz, yz interaction with p_2, p_3 of benzene is formally destabilizing, but due to the positive charge of the metal, the d AOs are low-lying, contracted, and thus give a weak overlap: the main covalent binding interaction now arises from 4s and 4p which are close to the π bonding MOs of benzene.

Singlet $[\text{Fe}(\text{C}_6\text{H}_6)]^{2+}$ ($e_2^4 a_1^2$) and triplet $[\text{Ni}(\text{C}_6\text{H}_6)]^{2+}$ ($e_2^4 a_1^2 e_1^2$) are isoelectronic to Cr^0 and Fe^0 complexes, respectively, but again with much more low-lying valence shells. Metal AOs are very contracted and leads to poor overlap: the covalent contribution of e_1 interactions are very weak. Thus the M–C bonds are weaker than in isoelectronic ${}^1\text{Cr}^0$ and ${}^3\text{Fe}^0$ complexes, respectively, and also weaker than in corresponding neutral ${}^3\text{Fe}^0$ and ${}^1\text{Ni}^0$ complexes. Nevertheless, e_1 interactions lead to a strong benzene-to-metal transfer. The ${}^1\text{Fe}^{2+}$ complex exhibits a slight C_{3v} chairlike distortion with alternation of shorter and longer C–C bonds. This phenomenon is significant at the 3-21G* level (1.415–1.434 Å) but becomes negligible at the DZVP2 level (1.4234–1.4236 Å). The large values of the bonding energies for these doubly charged species arises mainly from the transfer of about 0.5 electron (see Table 2) from benzene to low-lying metal levels.

Singlet $[\text{Ni}(\text{C}_6\text{H}_6)]^{4+}$, isoelectronic to the Fe^{2+} complex, was calculated to provide an example of a strong benzene to-metal-electron transfer. Indeed the results must be considered with some caution, since the DFT method and the basis set could be quite inaccurate in the calculation for highly charged species. In this complex we first note a marked C_{3v} distortion with a chairlike conformation of benzene (Figure 3), in which three carbon atoms bearing a positive charge are repelled from the metal, whereas the three other carbon atoms, closer to Ni, are nearly neutral. It is interesting to mention that no η^6 complex could be obtained in a quintet state, while a μ^1 complex is obtained for the triplet state.¹⁵

Ring Perturbation; Correlation between Benzene–Metal Electron Transfer and Bathochromic Shift of a CC Vibration Frequency. As characteristics of C–C bond strength, we refer to both bond length and to the $\nu_{\text{C–C}}$ vibration frequency which appears, for isolated benzene, as degenerate E_{1g} modes (modes 19A and 19B)¹⁶ at 1483 cm^{-1} : as a matter of fact, the corresponding absorption band (E_1 in C_{6v} complexes) is strong

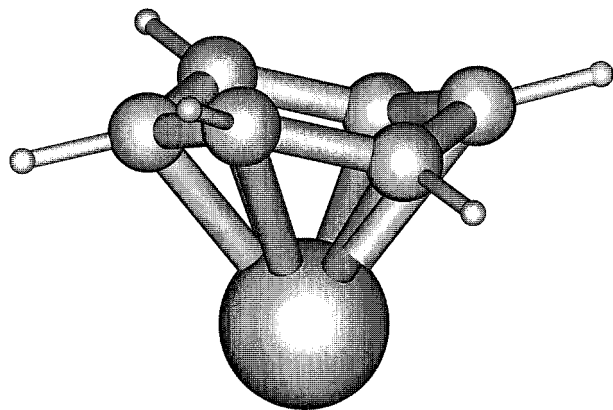


Figure 3. Optimized geometry of the $[^1\text{Ni}(\text{C}_6\text{H}_6)]^{4+}$ complex at the B3LYP/DZVP2 level.

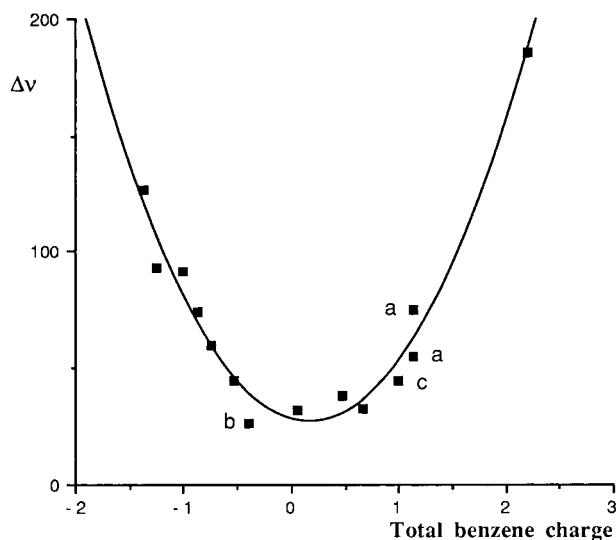


Figure 4. Bathochromic shift of the E_1 C–C vibration of metal–benzene complexes as a function of total benzene charge. (a) Nondegenerate values for $[^1\text{V}(\text{C}_6\text{H}_6)]^{3+}$; (b) $\text{Cr}(\text{CO})_3(\text{C}_6\text{H}_6)$; (c) C_6H_6^+ .

and can be easily observed experimentally. These data clearly depend on the electron-transfer balance between metal and benzene.

On one hand, the metal-to-benzene transferred electrons occupy the e_2 antibonding π_3^* , π_4^* levels, which weaken the C–C bonds. On the other hand, the benzene-to-metal electron transfer essentially occurs from the e_1 bonding π_2 , π_3 set, and results also in a weakening of C–C bonds. Finally, the total benzene Mulliken charge appears as a good index of the C–C bond weakening. As a matter of fact, this charge is nicely correlated to the bathochromic shift of the frequency associated to C–C stretching vibrations (Table 2 and Figure 4). The 3-21G* level has been used since, in a few cases, with the DZVP2 basis set, a stronger coupling between C–C stretching and C–H deformation modes yields perturbation in both frequency and relative intensities, which makes uncertain their assignment. On the other hand, this phenomenon could be at the origin of wrong experimental attributions (cf. infra). At the chosen level of calculation, B3LYP/3-21G*, the degenerate vibration has a frequency of 1525.5 cm^{-1} for isolated benzene. It is well-known that Mulliken charges must be considered with some caution, and these results are essentially qualitative trends. In this way, we can note that the greatest shifts occur for highly electron donor metals, such as Ti^0 , Cr^0 , and at the opposite for strong acceptors such as Fe^{2+} and Ni^{4+} . The weakest frequency shifts are encountered with $^3\text{Ni}^{2+}$ and $^1\text{Cu}^+$. The plot of Figure

4 is roughly symmetric, indicating that a positive or a negative transfer has almost the same result on the frequency shift. Experimental available results⁴ (Co^0 : -39 cm^{-1} and Ni^0 : -52 cm^{-1}) are in good agreement with calculated ones.

To obtain a benzene-to-metal charge-transfer value between those obtained with Fe^{2+} and Ni^{4+} we calculated the properties of singlet $[^1\text{V}(\text{C}_6\text{H}_6)]^{3+}$. This complex exhibits a non negligible C_{2v} distortion with a boatlike benzene and we thus report as simple landmarks, the nondegenerated ring vibrations (points (a) in Figure 4).

To verify that other benzenic systems undergo the same correlation, a calculation was performed on the $\text{Cr}(\text{CO})_3(\text{C}_6\text{H}_6)$ complex. A shift of -26 cm^{-1} has been calculated with a 0.390 benzene positive charge which fits with the preceding curve (B3LYP/3-21G*, point (b) in Figure 4). This shift value disagrees with the experimental reported value^{22(a)} of $+36\text{ cm}^{-1}$; this unexpectedly positive value could be explained by a strong coupling with C–H vibrations, which make difficult the assignment. It is worthy to note that for this vibration mode, a value of 1483 cm^{-1} , very close to our result (1482 cm^{-1}), has been reported on by Bércecs et al.^{22(b)}

In the isolated C_6H_6^+ cation, the degeneracy of the E_{1u} modes is raised, which gives rise, at the B3LYP/3-21G* level, to a low-frequency mode at 1482 cm^{-1} (point (c) in Figure 4), and a high-frequency one at 1559 cm^{-1} of weaker intensity.

In parallel, we note that longer C–C bonds, as compared to those of isolated benzene (1.397 \AA at the DZVP2 level) are encountered with large benzene absolute charges, either negative (1.447 with ^1Ti) or positive (1.469 in the $^1\text{Ni}^{4+}$ complex). In the latter case, the bond length (1.469 \AA) and the vibration frequency (1339 or 1337 cm^{-1} depending on the basis set) are closer to those of a single C–C bond than to an aromatic one.

Conclusion

The main qualitative trends in benzene–metal interaction in the series studied can be explained quite satisfactorily on the simple MO perturbation analysis. Nevertheless, a more quantitative analysis of the nature of the bonding using the ELF approach is in progress.¹⁵ From another point of view, most of the qualitative results reported here can hold true for supported metals such as Ni^+ or Ni^{2+} which can be described as tricoordinate complexes^{23,24} and thus interact with an additional ligand such as benzene mainly through a degenerate pair of d-type MOs. In addition, other systems that have not been considered in this work could be of interest, such as complexes which exhibit more or less marked Jahn–Teller distortions leading to flexible boatlike benzene rings in equilibrium through half-chairlike transition states.

References and Notes

- (1) Harman, W. D.; Taube, H. *J. Am. Chem. Soc.* **1988**, *110*, 7906; *ibid.* **1990**, *112*, 2682.
- (2) Pinnavaia, T. J.; Mortland, M. M. *J. Phys. Chem.* **1971**, *75*, 3957; Turner R. W.; Amma, E. L. *J. Am. Chem. Soc.* **1966**, *88*, 1877; Andrews, M. P.; Mattar, S. M.; Ozin, G. A. *J. Phys. Chem.* **1986**, *90*, 744.
- (3) Garrot, J.-M. Thèse de Doctorat de l'Université Pierre et Marie Curie, 1996; Garrot, J.-M.; Lepetit, C.; Che, M. *J. Mol. Catal. A* **1996**, *107*, 137.
- (4) Efner, H. F.; Tevault, D. E.; Fox, W. B.; Smardzewsky, R. R. *J. Organomet. Chem.* **1978**, *146*, 45.
- (5) *Organometallic Ion Chemistry*; Freiser, B. S., Ed.; Kluwer Academic Publishers: Dordrecht/Boston/London, 1996.
- (6) Marty, P.; de Parceval, P.; Klotz, A.; Serra, G.; Boissel, P. *Astron. Astrophys.* **1996**, *316*, 270.
- (7) Nicholas, J. B.; Hay, B. P.; Dixon, D. A. *J. Phys. Chem. A* **1999**, *103*, 1394.
- (8) Cubero, E.; Orozco, M.; Luque, F. J. *J. Phys. Chem. A* **1999**, *103*, 315.

- (9) Stöckigt, D. *J. Phys. Chem. A* **1997**, *101*, 3800; Silva, S. J.; Head, J. D. *J. Am. Chem. Soc.* **1992**, *115*, 9608.
- (10) Bauschlicher, C. W.; Partridge, H.; Langhoff, R. S. *J. Phys. Chem.* **1992**, *96*, 3273.
- (11) Yang, C.-N.; Klippenstein, S. J. *J. Phys. Chem. A* **1999**, *103*, 1094.
- (12) (a) Chuan-Yuan, L.; Chen, H.; Freiser, B. S. *J. Phys. Chem. A* **1997**, *101*, 6023. (b) Chuan-Yuan, L.; Dunbar, R. C. *Organometallic* **1997**, *16*, 2691.
- (13) Weiss, P.; Kemper, P. R.; Bowers, M. T. *J. Phys. Chem. A* **1997**, *101*, 8207; Hirano, M.; Judai, K.; Nakajima, A. *J. Phys. Chem. A* **1997**, *101*, 4893; Mattar, S. M.; Sammynaiken, R. *J. Chem. Phys.* **1997**, *106*, 1080–1093.
- (14) Schroeter, K.; Wesendrup, R.; Schwartz, H. *Eur. J. Org. Chem.* **1998**, *4*, 565.
- (15) Chaquin, P.; Costa, D.; Lepetit, C.; Che, M. Work in progress.
- (16) Herzberg, G. *Infrared and Raman Spectra of Polyatomic Molecules*; Van Nostrand Reinhold Company: New York, 1966.
- (17) Frisch, M. J.; Trucks, G. W.; Schlegel, H. B.; Gill, P. M. W.; Johnson, B. G.; Robb, M. A.; Cheeseman, J. R.; Keith, T.; Petersson, G. A.; Montgomery, J. A.; Raghavachari, K.; Al-Laham, M. A.; Zakrzewski, V. G.; Ortiz, J. V.; Foresman, J. B.; Cioslowski, J.; Stefanov, B. B.; Nanayakkara, A.; Challacombe, M.; Peng, C. Y.; Ayala, P. Y.; Chen, W.; Wong, M. W.; Andres, J. L.; Replogle, E. S.; Gomperts, R.; Martin, R. L.; Fox, D. J.; Binkley, J. S.; Defrees, D. J.; Baker, J.; Stewart, J. P.; Head-Gordon, M.; Gonzalez, C.; Pople, J. A. *Gaussian 94*, revision B.1; Gaussian, Inc.: Pittsburgh, PA, 1995.
- (18) Becke, A. D. *J. Chem. Phys.* **1993**, *98*, 5648.
- (19) Lee, C.; Yang, W.; Parr, R. G. *Phys. Rev. B* **1988**, *37*, 785.
- (20) Godbout, N.; Salahub, D. R.; Andselm, J.; Wimmer, E. *Can. J. Chem.* **1992**, *70*, 560.
- (21) Davidson, E. R. *Int. J. Quantum Chem.* **1998**, *69*, 241.
- (22) (a) Adams, D. M.; Christopher, R. E.; Stevens, D. C. *Inorg. Chem.* **1975**, *14*, 1562. (b) Bérces, A.; Ziegler, T. *J. Phys. Chem.* **1994**, *98*, 13233.
- (23) Garrot, J. M.; Lepetit, C.; Che, M.; Chaquin, P. *J. Phys. Chem. A.*, submitted.
- (24) Costa, D.; Kermarec, M.; Che, M.; Girard, Y.; Chaquin, P. *New Trends in Quantum Systems in Chemistry and Physics*; Kluwer: Dordrecht, 2000; Vol. 2, pp 257–268.